Scrap tire pyrolysis: experiment and modelling

A. Napoli, Y. Soudais, D. Lecomte
Ecole des Mines d'Albi - Carmaux
Centre Energétique-Environnement
Campus Jarlard - route de Teillet
81 013 Albi - FRANCE

S. Castillo
Laboratoire Matériaux et Energie
Université Paul Sabatier
118, route de Narbonne
31 062 Toulouse - FRANCE

INTRODUCTION

Pyrolysis of waste, usually organic solids like tires, plastics or composite materials, is an alternative thermal waste treatment technology. Three main physical and chemical mecanisms -i.e.: chemical kinetics, internal heat transfer and external heat transfer - have to be considered when modelling the degradation of solid waste particles. Because of the lack of physical properties for wastes most of the models described in the literature use basic data obtained on the pyrolysis of coal, wood and biomass. In this work, we report basic information on the thermal degradation of tire samples at small scale: Thermogravimetric analyser (TGA) and differential scanning calorimeter (DSC), as well as direct and indirect measurements of thermal and physical properties (thermal conductivity of the tire and of the char, porosity, density, specific heat). Pyrolysis experiments on tire samples are performed in an imaging furnace. The experimental results are compared to theoretical values deduced from models that take into account physical property measurements.

ANALYSIS

Works on the pyrolysis of coal, wood and biomass have led to numerous model descriptions taking into account heat and mass transfer in large solide particles undergoing pyrolysis reactions. Pyle and Zaror[1] studied two major dimensionless groups: the Biot number (Bi) which compares external convection and internal conduction and the Pyrolysis number (Py), which compares internal heat conduction transfer and chemical kinetics. Internal convection is assumed negligible and external heat transfer (convection and radiation) may be described by a third-order boundary condition. Based on this analysis, simplified models can be developed for design or modelling of reactors. A fundamental study of wood pyrolysis by Kansa and co-authors[2] takes into account heat conduction, internal convection, mass, energy and momentum equations for the solid and the released gas. The influence of the Peclet number (Pe), which compares internal conduction and internal convection, is studied. In most pyrolysis models, internal convection is neglected.

Chemical kinetics

The pyrolysis reaction in a solid (wood, biomass particle, coal, etc.) is described by many authors[1,3-5] as a source term in the local energy equation:

$$p = -\Delta H \frac{\partial \rho_s}{\partial t} \qquad (1)$$

where

p = source term in $W.m^{-3}$

ΔH = overal heat of reaction during the pyrolysis process in $J.kg^{-1}$

$\frac{\partial \rho_s}{\partial t}$ = local mass loss in $kg.m^{-3}.s^{-1}$

The local mass loss is determined from the overall mass loss obtained by TGA. Several methods are described to determine the kinetic law from non-isothermal thermogravimetric analyser (TGA) measurements[6]. Other authors[1-2] assume a simple Arrhenius decomposition equation :

$$\frac{\partial \rho_s}{\partial t} = -A e^{\frac{-E}{RT}} (\rho_s - \rho_{s\infty})^n \qquad (2)$$

where

A	=	frequency factor in s^{-1}
E	=	activation energy in $J.mol^{-1}$
R	=	gas constant in $J.mol^{-1}.K^{-1}$
T	=	temperature in K
ρ_s	=	density of the solid at a time t in $kg.m^{-3}$
$\rho_{s\infty}$	=	density of the solid at the end of the pyrolysis reaction in $kg.m^{-3}$
n	=	order of the reaction

In the case of waste, which are multi-component and heterogeneous materials, little information is available on the chemical reactions involved in pyrolysis. The basic TGA and DSC measurement methods provide a global information about heat and mass balance on a small sample of the material. Some of the reactions may be exothermic, others endothermic, according to the temperature range. Yang and co-authors[7] studied the degradation of the elastomers which are the main degradable components of waste tires : styrene-butadiene rubber (SBR), polybutadiene rubber (BR) and natural rubber (NR). The mass loss is the algebric sum of the mass losses of the elastomers:

$$\frac{\partial \rho_s}{\partial t} = \sum_i \frac{\partial \rho_i}{\partial t} \qquad (3)$$

where

$\frac{\partial \rho_i}{\partial t}$	=	local mass loss of component i in $kg.m^{-3}.s^{-1}$

A first order kinetic equation is used to describe the reaction kinetics :

$$\frac{\partial \rho_i}{\partial t} = -A_i e^{\frac{-E_i}{RT}} \rho_i = K_i \rho_i \qquad (4)$$

where

A_i	=	frequency factor of the component i in s^{-1}
E_i	=	activation energy of the component i in $J.mol^{-1}$
K_i	=	rate constant of the component i in s^{-1}
ρ_i	=	density of the component i at a time t in $kg.m^{-3}$

Kim and co-authors[8] calculate K_i and $\frac{\partial \rho_s}{\partial t}$ by fitting the TGA data with Equation (3). The method requires no preliminary investigation about the initial material composition. It is assumed that tire rubber is constituted of various compounds which undergo independant decomposition reaction in characteristic individual temperature regions. Each decomposition is governed by a first order irreversible independant reaction and the kinetic parameters were obtained by differential methods[9-10]
Even with a realistic description of the mass loss term as a function of temperature, Equation (1) does not take into account the thermal effects at different temperatures.

For waste tire pyrolysis, degradation exhibits an exothermic reaction between two endothermic stages[11-12]. Mass loss occurs at 200°C, but thermal degradation (softening and liquefaction) starts almost at ambient temperature. It is thus important to have a better description of the source term used in the energy equation.

Yang and co-authors[11] make a clear distinction between the source term induced by thermal degradation (no mass loss) and the source term induced by volatilization of the elastomers. The heat release process is described by a simulative curve of the DTA and DSC enthalpy measurements.
The decomposition source term without mass loss is expressed as :

$$p_d = \sum h_{di} \rho_i \frac{d\alpha_i}{dt} \quad (5)$$

where

h_{di} = heat of reaction of component i in $J.kg^{-1}$

$\frac{d\alpha_i}{dt}$ = rate of decomposition of component i in s^{-1}

ρ_i = density of component i in $kg.m^{-3}$

The evaporation source term is expressed as :

$$p_v = \sum h_{gi} \frac{d\rho_i}{dt} \quad (6)$$

where

h_{gi} = latent heat of component i in $J.kg^{-1}$

$\frac{d\rho_i}{dt}$ = rate of weight loss of component i $kg.m^{-3}s^{-1}$

Heat transfer

When the Pyrolysis number is small, the pyrolysis process is controlled by internal or external heat transfer. The heat transfer problem is often treated as a moving boundary problem[13]. Among the models which were developped for wood and biomass pyrolysis, integral balance techniques provide approximate analytical solutions[14]. For internal controlled processes (small Biot number), pyrolysis rate is very sensitive to thermal conductivity and a good prediction of the pyrolysis time requires an accurate knowledge of the conductivity of the material and of the char. In the case of waste or heterogeneous materials, little information on the thermal conductivity is available. For the char, the conductivity is dependant on the structural properties of the material itself. The wood-cell arrangement generates a pseudo-periodic porous char. For tire particles, evaporation occurs in two-phase porous medium made of liquid elastomers and solid carbon black. This 'bubbling' mechanism[15] generates microporosity in the char.
The conduction term in the energy equation can be written :

$$q = -\nabla.(k^* \nabla T) \quad (7)$$

where

k^* = apparent thermal conductivity in $W.m^{-1}.K^{-1}$

∇ = gradient (vector) differential operator equivalent to a partial derivative in a one dimensional system

A review of thermal conductivity models in porous media was made by Azizi[16]. The apparent thermal conductivity is influenced by the conductivity of the two phases and the proportion of the phases (porosity). But the influence of geometry is important and more information about the microscopic arrangement of the carbon black in the porous structure is needed for a correct description of conductive heat flow. In the litterature about pyrolysis models, the parallel model in which the thermal conductivity

is assumed to be linearly dependent of the various phases conductivity, is often used without justification[11]. For large temperature gradients, internal radiative transfer must be considered.

EXPERIMENTS

Kinetics

The experiments were performed with a Calvet-type heat flow Differential Scanning Calorimeter (Setaram DSC 111) coupled with a thermobalance (Setaram ATG 92). The reference material was a fixed amount of a-alumina. The powder tire samples were obtained by cryogenic grinding device (SPEX 6700 Freezer/Mill) giving a particle size range of 100-250 μm small enough to ensure internal isothermal conditions during experiments. A flow of purified argon in both the reference and the sample tube was used to maintain an inert atmosphere and to remove the volatile products. The tire samples were studied from 30°C to 800 °C at a heating rate of 5°C.min^{-1}. The final temperature was maintained for one hour to obtain a complete pyrolysed solid (char). Two experiments were realized in the same conditions with the char and the empty crucible respectively in order to record the char and blank signals. Mass loss curves and mass loss rate curves were continuously measured in each experiment.

Thermal diffusivity measurements

The flash method[17-18] was used to measure the thermal diffusivity of tire and char. A brief thermal impulsion is absorbed on the upper side of the sample and the consequent temperature increasing on the back side is recorded. The sample is maintained in a tubular furnace and measurements can be obtained at various temperature from ambient temperature to 300°C. The measurement requires a disc sample of 30 mm diameter, 4 mm thickness with the two faces parallel (Figure 1).

Imaging furnace

An imaging furnace described elsewhere[19] (Figure 2) was used as the experimental device to study the internal thermophysical tire properties. A Xenon arc lamp (4,5 kW) is the radiative source of energy. Spheric and elliptic mirrors concentrate the flux at the focus of the furnace. The sample (12 mm diameter, 3 mm thickness pellet) lies on the top of a sliding support allowing to lead it to the focus where its upper side is exposed to the high radiative flux while its lower side is insulated. The carrier gas (N_2, 200 mL.min^{-1}) is swept under the quartz cover (60 mm diameter, 60 mm high) to maintain neutral atmosphere (Figure 3). The time of treatment is easily controlled by the mean of the sliding support. The high energy supplied by the imaging furnace allows a great gradient of temperature to establish inside the solid; otherwise, as a high temperature is quickly reached in the solid, we can assume that the pyrolysis kinetic is not a limitative factor. So, the boundary conditions are easily controlled in this furnace and the reaction rate may be neglected regarding to the internal heat transfer. This experimental device allows to study the internal heat transfer in a solid chip submitted to a pyrolysis reaction.

MODEL

The mass and energy balance equations for a material undergoing pyrolysis reactions may be written :

mass balance

$$\frac{\partial \rho_s}{\partial t} + \nabla.(\rho_g \mathbf{v}) = 0 \qquad (8)$$

energy balance

$$\frac{\partial}{\partial t}\left[\rho_g u_g + \rho_s u_s\right] + \nabla.(\rho_g u_g \mathbf{v}) = \nabla.(k^* \nabla T) + \frac{-\partial \rho_s}{\partial t}.(h_g - h_s) \quad (9)$$

where

ρ_g = apparent density of gas in $kg.m^{-3}$

ρ_s = apparent density of solid in $kg.m^{-3}$

u_s, h_s = internal energy, enthalpy of solid in $J.kg^{-1}$

u_g, h_g = internal energy, enthalpy of gas in $J.kg^{-1}$

$\mathbf{v}$ = Darcy velocity of gas in $m.s^{-1}$

k^* = thermal conductivity of the solid in $W.m^{-1}.K^{-1}$

Assuming convection negligible ($\mathbf{v} = 0$), Equation (9) becomes:

$$\frac{\partial}{\partial t}(\rho_g u_g + \rho_s u_s) = \nabla.(k^* \nabla T) + (-\frac{\partial \rho_s}{\partial t})(h_g - h_s) \quad (10)$$

Assuming $\rho_g u_g << \rho_s u_s$, we obtain :

$$\frac{\partial(\rho_s u_s)}{\partial t} = \nabla.(k^* \nabla T) + \frac{-\partial \rho_s}{\partial t}.(h_g - h_s) \quad (11)$$

The internal energy u_s is the sum of the latent heat L_s and the sensible heat $c_s T$:

$$\frac{\partial(\rho_s c_s T)}{\partial t} = \nabla.(k^* \nabla T) - L_s \rho_s \frac{\partial \alpha}{\partial t} + \frac{-\partial \rho_s}{\partial t}.(h_g - h_s) \quad (12)$$

where

$\frac{\partial \alpha}{\partial t}$ = rate of solid-liquid transformation of the solid ($0 < \alpha < 1$) in s^{-1}

The Pyrolysis number can be defined by :

$$P_y = \frac{k^*}{K \rho_s c_s l^2} \quad (13)$$

where

K = the lowest constant rate for the pyrolysis reactions in s^{-1}

l = dimension of sample in m

Assuming $P_y << 1$, the controlling factor is heat transfer and thus the quantities α, $h_g - h_s$ and $\frac{\partial \rho_s}{\partial t}$ in Equation (12) are only dependent on temperature T.

To solve Equation (12), an integral balance method can be used (in the 1 dimensional case)

$$\int_D \frac{\partial \rho_s c_s T}{\partial t} dx = \int_D \nabla.(k^* \nabla T) dx + \int_D -\frac{\partial \rho_s}{\partial t}(h_g - h_s) dx + \int_D -\frac{\partial \alpha}{\partial t} L_s \rho_s dx \quad (14)$$

where

D = domain of integration (thickness of material which changes over time)

A simplified expression of $\int_D -\frac{\partial \rho_s}{\partial t}(h_g - h_s)dx + \int_D -\frac{\partial \alpha}{\partial t}L_s\rho_s dx$ is given by Kanury and Holve[14] assuming a constant pyrolysis temperature T_c with constant bulk enthalpy change ΔH. Equation (14) reduces to :

$$\frac{\partial}{\partial t}\int_D \rho_s c_s T dx = \int_D \vec{\nabla}.(k^* \nabla T)dx + (\rho_c - \rho_0)\Delta H \frac{dx_c}{dt} \quad (15)$$

where x_c, ρ_c, ρ_0 are defined in Table 1

The boundary conditions are :
- constant radiative heat flux at x=0
- no heat loss at x=l

The solution of this integral equation is given by Kanury and Holve[14] with the following assumptions :
- The thermophysical properties are independent of temperature but depending on density. The properties of non reacted solid are noted with subscript 0 whereas the properties of char are noted with subscript c.
- A linear temperature profil is chosen to integrate the energy balance along the x axis.

The model describes the pyrolysis reactions as a three main phase process: a preheated phase (Figure 4a) corresponds to the increase of the temperature from T_i up to T_c into the depth x_t; an early-charring (Figure 4b) phase where a continuously thickening char layer x_c exists near the exposed surface and a thermal wave x_t propagates into the solid; and a late-charring (Figure 4c) phase where the char front x_c propagates across the solid to the insulated face.
The basic equations of the model are reported in Table 1.

RESULTS AND DISCUSSION

Kinetics

Typical TGA, DTG (derivative thermogravimetry) and DSC results are illustred on Figure 5 and Figure 6 respectively.
The major composite materials of tire rubber are carbon black, elastomers and processing oils[7,12].
Three stages of degradation are easily recognized on the DTG curve. Brazier and al.[20] attributed the first stage of degradation (150-310 °C) to the evaporation of oil/plastizer included in the tire. The second and third stages correspond to the degradation of elastomers. The temperature of degradation of natural or polyisoprene rubber is about 373 °C while styrene-butadiene copolymers rubber decompose on the 430-450 °C temperature range depending on styrene content. The total weight loss is more than 60 % of the initial mass and the remaining char is constituted of inert carbon black and ash. The thermal degradation takes place between 280-480 °C and is achieved when the temperature reached 500 °C. A pyrolysis temperature T_c of 380 °C was choosen for the Kanury model[14].

The DSC curve on Figure 6 shows an endothermic process at the beginning of the treatment, an exothermic transition between 300-400 °C and finally an endothermic process up to 500 °C. The endothermic energy may be due to the rupture of chemical bonds in the polymer leading to a viscous

aspect. Sircar and al.[12] attribute the exothermic transition to bond-forming reactions like crosslinking, cyclization. The ΔH reaction energy is calculated in the total range of the study and the value of 713 $kJ.kg^{-1}$ is used in the model. The specific heat of tire is measured in the degradation region 30°C-200°C and a mean value of $c_0 = 1417\ J.kg^{-1}.K^{-1}$ is chosen. The specific heat of char is determined in the high temperature region 380°C-800°C where the solid is completely degraded. The value of $c_c = 1779\ J.kg^{-1}.K^{-1}$ is retained for the model.

Thermal diffusivity measurements

Measurements were made with the flash method both for the tire sample and the char. Values are reported in Table 2

To obtain a good measurement, the shape of the sample should be perfectly cylindrical with plane and parallel faces. But during the pyrolysis process, warping and splitting of the sample may be observed especially at high temperature and high heat flux. An important volume change may in some case be observed (up to twice the initial volume). To obtain correct shaped samples, a tubular electrical furnace was used with mild external conditions. The values of thermal diffusivity were given for ambient temperature. Effets of high temperature and radiation were not studied in this experiment.

Imaging furnace

Experimental results are shown on Figure 7. The overall mass loss of a tire sample is plotted versus time when undergoing a high constant heat flux (100 $W.cm^{-2}$) on one face, the other face being insulated. With this very severe external conditions, temperature rise in the sample is very fast and the main limiting phenomen on is internal heat transfer. Comparison between the model and experience points out the influence of thermal conductivity of the solid char on the duration of pyrolysis. The values taken in the model and reported from the experiments described above are recorded in Table 2. The experimental data may be fitted by a theoretical value $k_c = 0.085\ W.m^{-1}.K^{-1}$, noticeably different from the measured value $k_c = 0.14\ W.m^{-1}.K^{-1}$. Several explanations may be given for this discrepancy : the conditions of pyrolysis were different between the imaging furnace and the electrical tubular furnace which was used to prepare the samples. As a matter of fact, high thermal rates may cause greater volume change ("pop corn effects") and increase porosity inside the char thus lowering the apparent thermal conductivity. The existence of cracks and splits may also have identical effects on the char thermal conductivity.

CONCLUSION

Little data on the thermophysical properties of waste is available. This paper points out the importance of these data in the energy equation : heat of reaction, heat of vaporization, overall enthalpy, reaction kinetics, specific heat, thermal conductivity, temperature range of pyrolysis.

A preliminary set of measurement techniques was presented in the present paper with a special interest on scrap tire pyrolysis. The following results were obtained :

1. Combined DSC and TGA is a powerful technique to take into account mass and energy balances in the pyrolysis reactions. Mass losses, but also overall reaction enthalpy, specific heat of waste and char may be obtained. Thermal effects, endothermic and exothermic, may be observed and put in relation with mass losses.

2. For large tire particles, heat conduction is a dominant effect on the overall behaviour of the pyrolysis reaction, but the determination of thermal diffusivity is not straightforward. According to the experiments described the order of magnitude of the thermal conductivity is 0.085 - 0.14 $W.m^{-1}.K^{-1}$ depending on the pyrolysis process. These very low values show that char is a very insulating material.

The results presented show the importance of a thorough characterization of solid wastes with respect to pyrolysis processes. Heat conductivity, specific heat and heat of reactions have a strong influence on the overall energy balance as well as the characteristic times of the process. A complete model including competition between internal and external heat transfer effects, reactions kinetics, temperature range effects, based on accurate determination of thermophysical parameters is currently developed and will be presented soon.

1. D.L. Pyle and C.A. Zaror, "Heat transfer and kinetics in the low temperature pyrolysis of solids," Chem. Eng. Sci., 39(1): 147 (1984)

2. E.J. Kansa, H.E. Perlee and R.F. Chaiken, "Mathematical model of wood pyrolysis including internal forced convection," Combust. Flame, 29: 311 (1977)

3 H.C. Kung, "A mathematical model of wood pyrolysis," Combust. Flame, 18: 185 (1972)

4 Z. Pan, H.Y. Feng and J.M. Smith "Rates of pyrolysis of Colorado oil shale," A.I.CH.E. J., 31: 721 (1985)

5 C.A. Koufopanos, N. Papayannakos, G. Maschio and A. Lucchesi "Modelling of the pyrolysis of biomass particles. Studies on kinetics, thermal and heat transfer effects," Can. J. Chem. Eng., 69: 907 (1991)

6 W.W. Wendlandt, Thermal analysis, 3rd ed., John Wiley & Sons, New York, 1986, pp 57-82.

7 J. Yang, S. Kaliaguine and C. Roy "Improved quantitative determination of elastomers in tire rubber by kinetic simulation of DTG curves," Rubber Chem. Technol., 66(2): 213 (1993)

8 S. Kim, J.K. Park and H.D. Chun "Pyrolysis kinetics of scrap tire rubbers. I: using DTG and TGA," J. Environ. Eng., july: 507 (1995)

9 J.H. Flynn and L.A. Wall "General treatment of the thermogravimetry of polymers," J. Res. Nat. Bur. Standard, 70A(6): 487 (1966)

10 P. Kofstad "Oxidation of metals: determinatuion of activation energies," Anal. Chem., 179(Jun. 29): 1362 (1957)

11 J. Yang, P.A. Tanguy and C. Roy "Heat transfer, mass transfer and kinetics study of the vacuum pyrolysis of a large used tire particle," Chem. Eng. Sci., 50(12): 1909 (1995)

12 A.K. Sircar and T.G. Lamond "Identification of elastomers by thermal analysis," Rubber Chem. Technol., 345: 329 (1972)

13 R.E. Desrosiers and R.J. Lin "A moving-boundary model of biomass pyrolysis," Sol. Energy, 33(2): 187 (1984)

14 A.M. Kanury and D.J. Holve "Transient conduction with pyrolysis (Approximate solutions for charring of wood slabs)," J. Heat Trans., 104: 338 (1982)

15 A. Attar "Bubble nucleation in viscous material due to gas formation by a chemical reaction: application to coal pyrolysis," A.I.Ch.E. J., 24(1): 106 (1978)

16 S. Azizi : "Conductivité thermique des matériaux poreux humides : mesure par méthode flash et interprétation", Thesis INPL, 25 Mars 1988, Nancy, France.

17 A. Degiovanni "Diffusivité et méthode flash," Rev. Gén. Ther., 185: 420 (1977)

18 W.J. Parker, R.J. Jenkins, G.P. Buttler, G.L. Abbott "Flash method of determining thermal diffusivity heat capacity and thermal conductivity," J. Appl. Phys., 32(9) (1961)

19 S. Bennini, S. Castillo, J.P. Traverse "Effects of an intense thermal flux on a lignocellulosic material," J. A. A. P., 21: 305 (1991)

20 D.W. Brazier and G.H. Nickel "Thermoanalytical methods in vulcanizate analysis II. Derivative thermogravimetric analysis," Rubber Chem. Technol., 48: 661 (1975)

Table 1. Kanury and al. model

Phase	Mathematical model	Comments
Adimensional variables	$\theta \equiv \frac{T - T_i}{T_c - T_i}$ $\xi \equiv \frac{x}{l}$ $\tau \equiv \frac{\alpha_0 t}{l^2}$ $\sigma \equiv \frac{\rho_c c_c}{\rho_0 c_0}$ $\bar{q} \equiv \frac{\dot{q}_s'' l}{k_0 (T_c - T_i)}$ $\lambda \equiv \frac{\Delta H (\rho_0 - \rho_c)}{\rho_0 c_0 (T_c - T_i)}$ $\kappa \equiv \frac{k_c}{k_0}$	T_i initial temperature in K T_c pyrolysis temperature in K x abscisse in m l depth of solid in m $\alpha_0 = \frac{k_0}{\rho_0 c_0}$ thermal diffusivity of tire in $m^2.s^{-1}$ t time in s k_0 thermal conductivity of tire in $W.m^{-1}.K^{-1}$ k_c thermal conductivity of char in $W.m^{-1}.K^{-1}$
Preheated phase $0 \le \tau \le \tau_0$	$\xi_T(\tau) = \sqrt{2}\tau$ $\xi_c(\tau) = 0$	
Early-Charring phase $\tau_0 \le \tau \le \tau_s$	$\xi_c(\tau) = \frac{\kappa\lambda}{\sigma\bar{q}} \left(\sqrt{1 + \frac{2\sigma\bar{q}}{\kappa\lambda^2} \left(\bar{q}\tau - \frac{F(\tau)}{2} \right)} - 1 \right)$ with $F(\tau) \equiv \sqrt{4\left(\tau - \frac{1}{2\bar{q}^2}\right) + \frac{1}{\bar{q}^2}}$	ΔH enthalpy of pyrolysis reaction in $J.kg^{-1}$ $\dot{q}_s''$ heat flux on the upper side of solid in $W.m^{-2}$ ρ_c density of char in $kg.m^{-3}$ ρ_0 density of tire in $kg.m^{-3}$ x_c abscisse of the char front in m
Late-Charring phase $\tau_s \le \tau$	$\xi_c(\tau) = \frac{\kappa\lambda}{\sigma\bar{q}} \left(\sqrt{1 + \frac{2\sigma\bar{q}}{\kappa\lambda^2} \left(\left(\bar{q} - \frac{1}{1 - \xi_{cs}} \right) (\tau - \tau_s) + \lambda\xi_{cs} + \frac{\sigma\bar{q}}{2\kappa} \xi_{cs}^2 \right)} - 1 \right)$ with $\xi_{cs} = \xi_c(\tau_s)$	

Table 2. Property values used in the Kanury and al. model

	Tire	Char	Reference
Conductivity ($W.m^{-1}.K^{-1}$)	0.35	0.14	Flash method
Specific heat ($J.kg^{-1}.K^{-1}$)	1417	1779	DSC
density ($kg.m^{-3}$)	1100	479	Yang[11]
Pyrolysis temperature T_c (K)	653		ATG
Heat of Pyrolysis ΔH ($kJ.kg^{-1}$)	713		DSC
Radiative Flux $\dot{q}_s''$ ($W.m^{-2}$)	10^6		
Depth of solid l (m)	$3\ 10^{-3}$		

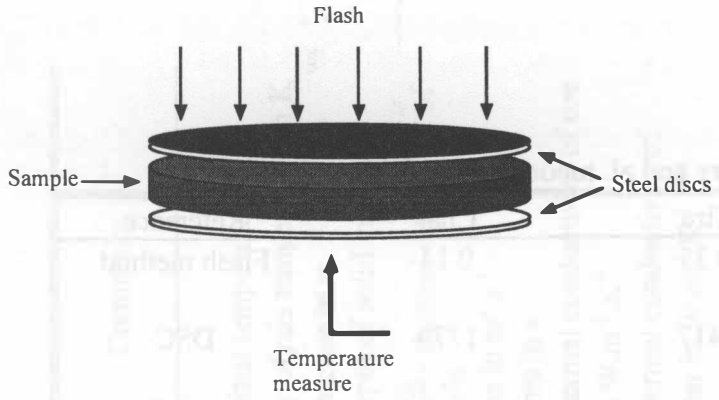

Figure 1. Schematic device of thermal diffusivity measurement by the flash method

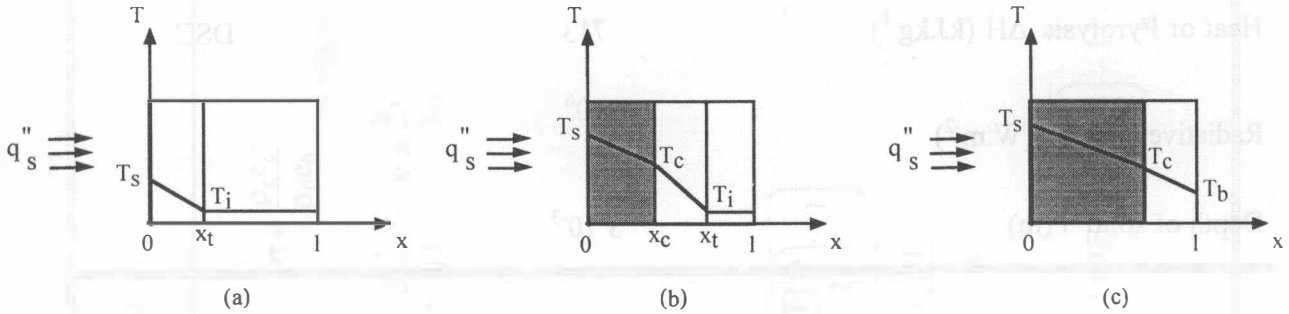

Figure 4. Schematic representation of the Kanury and al. model

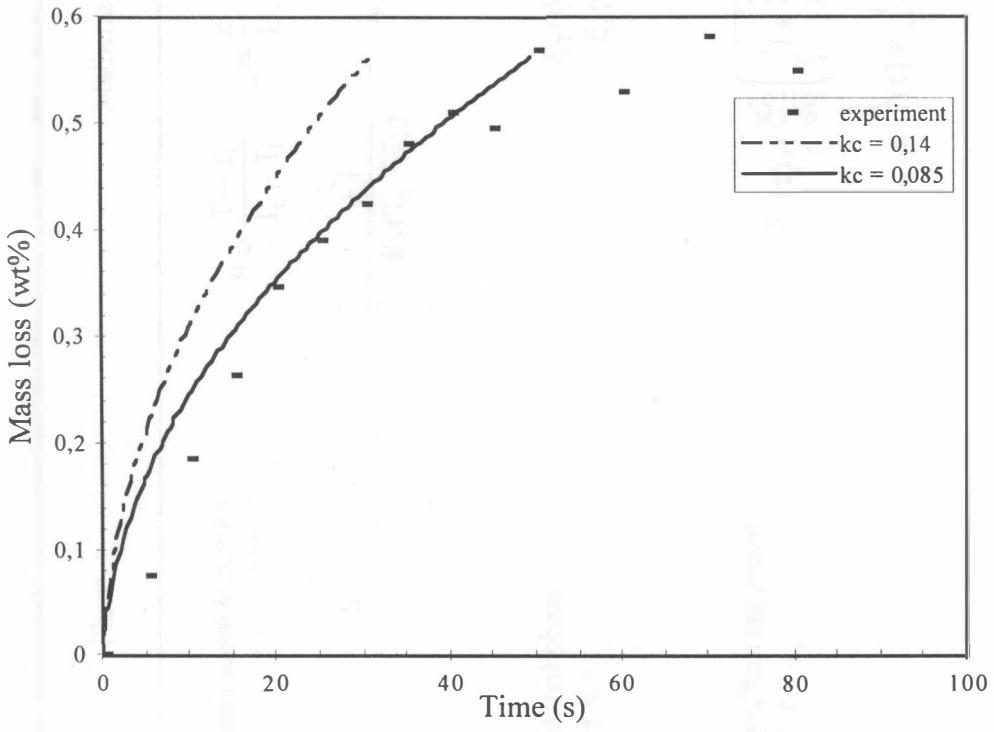

Figure 7. Mass loss vs. time : experimental results (imaging furnace); Kanury and al. model (kc=0.14 and 0.085 $W.m^{-1}.K^{-1}$)

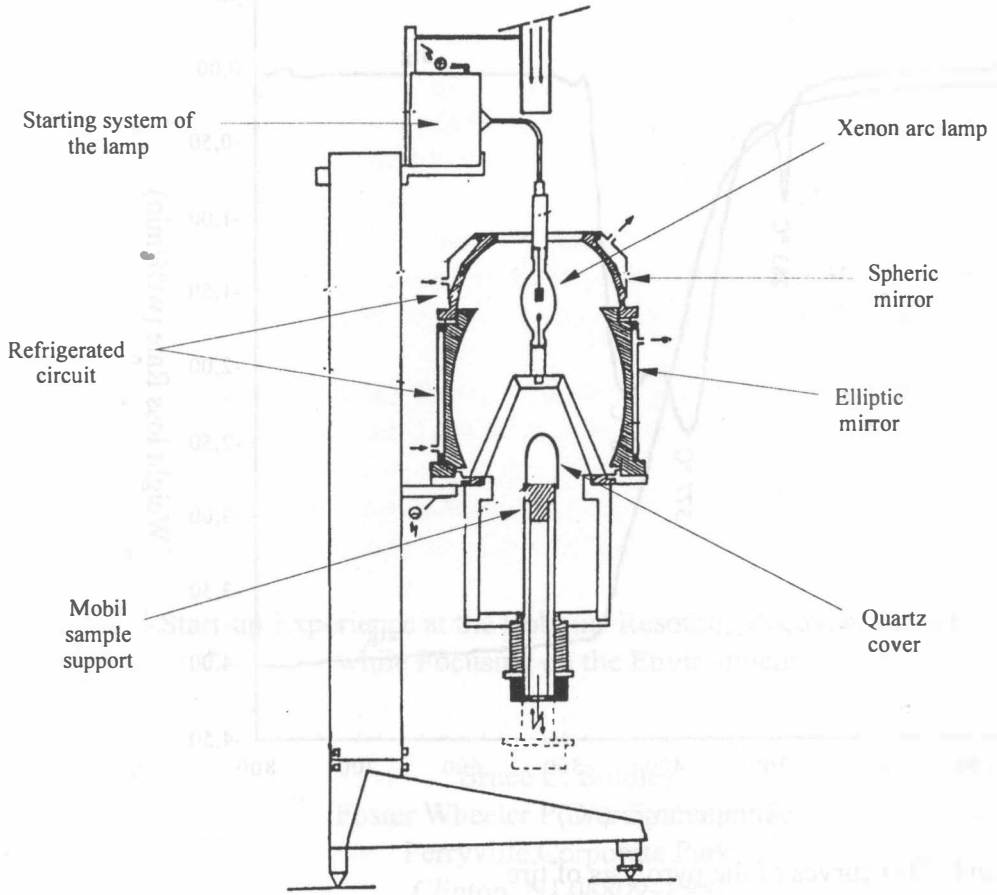

Figure 2. Imaging furnace

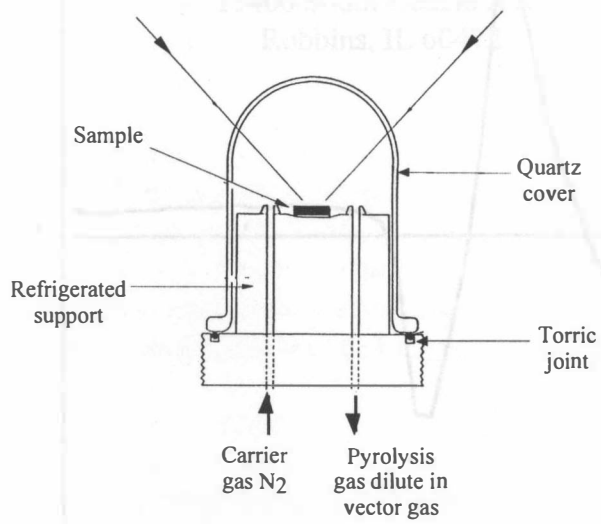

Figure 3. Detailled quartz cover

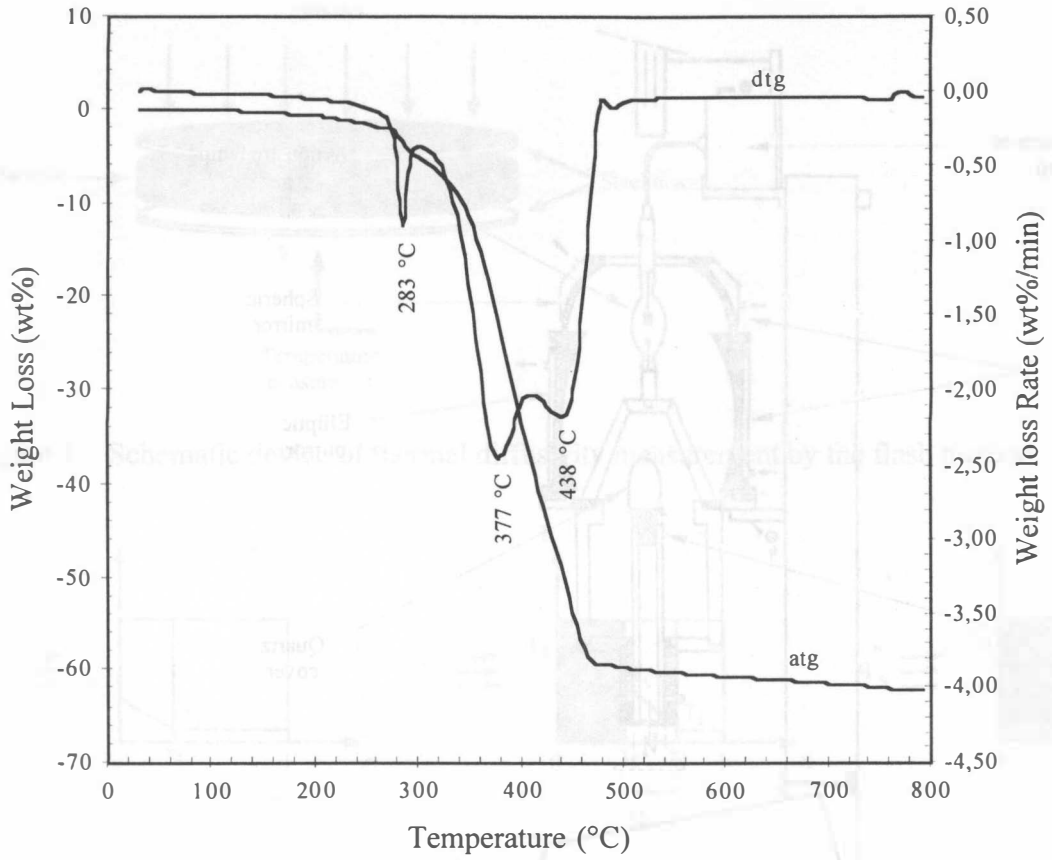

Figure 5. ATG and DTG curves of the pyrolysis of tire

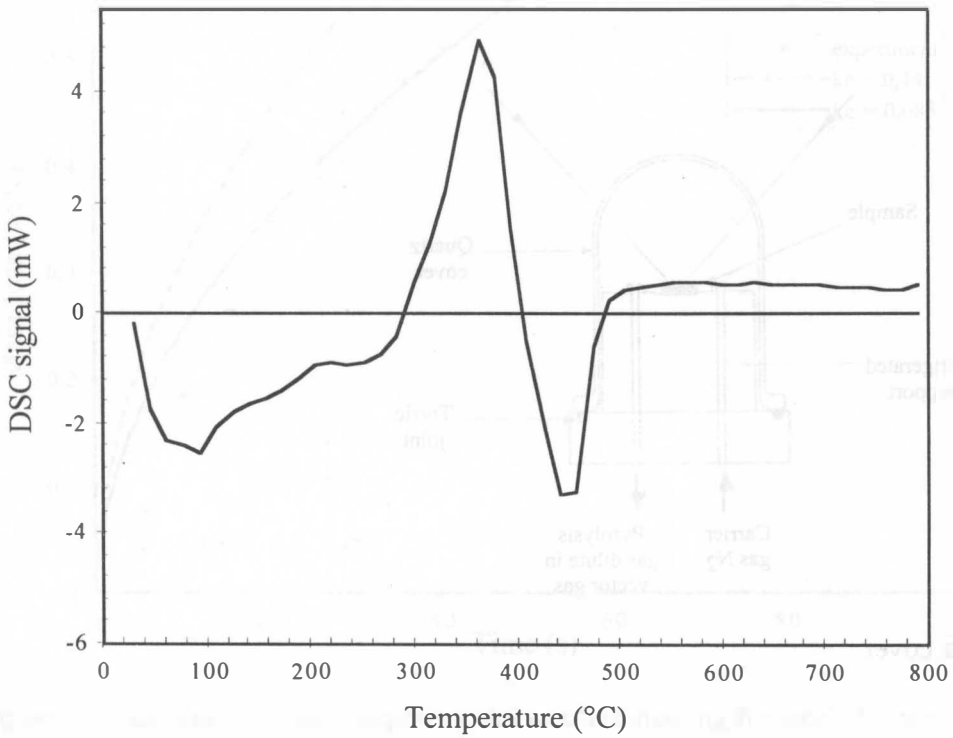

Figure 6. DSC curve of the pyrolysis of tire